SCIENCE CHINA
Information Sciences

• **Supplementary File** •

Movable Antennas for THz Multicasting: Grating-Lobe Analysis and Position Optimization

Ke Liu[1], Xin Wei[1], Weidong Mei[1*], Xinhang Wei[2], Zhi Chen[1] & Boyu Ning[1]

[1]*National Key Laboratory of Wireless Communications, University of Electronic Science and Technology of China, Chengdu 611731, China;*
[2]*Glasgow College, University of Electronic Science and Technology of China, Chengdu 611731, China*

Appendix A Grating-Lobe Analysis

To facilitate the analysis, we assume that the size of the transmit region (i.e., A) is sufficiently large, such that constraint (3b) can be relaxed. Note that to maximize the received signal power at any specific user (e.g., user 1), the transmit beamforming should be set based on the maximum ratio transmission (MRT) as

$$\boldsymbol{w}(\boldsymbol{T}) = \sqrt{P_{\max}} \frac{\boldsymbol{h}_1(\boldsymbol{T})}{||\boldsymbol{h}_1(\boldsymbol{T})||}. \tag{A1}$$

Next, we show that the MRT in (A1) for user 1 can also lead to the maximum beamforming gain at any other user k, $k \in \mathcal{K}^c = \mathcal{K}\backslash\{1\}$ under certain conditions. By substituting (A1) into (2), the received SNR at user k is expressed as

$$\gamma_k(\boldsymbol{T}) = \frac{\beta P_{\max}}{N d_k^2 \sigma_k^2} \left| \sum_{n=1}^{N} e^{j(x_n a_k + y_n b_k)} \right|^2, \forall k \in \mathcal{K}^c, \tag{A2}$$

where

$$a_k = \frac{2\pi}{\lambda}(\sin\theta_1 \cos\phi_1 - \sin\theta_k \cos\phi_k), \forall k \in \mathcal{K}^c, \tag{A3}$$

$$b_k = \frac{2\pi}{\lambda}(\cos\theta_1 - \cos\theta_k), \forall k \in \mathcal{K}^c. \tag{A4}$$

To proceed, we present the following theorem.

Theorem A1. Let $\tau_k = \lambda a_k / 2\pi = \sin\theta_1 \cos\phi_1 - \sin\theta_k \cos\phi_k$, $k \in \mathcal{K}^c$. If all τ_k's are rational numbers, there must exist an APV $\boldsymbol{T}^\star$ such that the maximum beamforming gain can be achieved at each user in $\mathcal{K}^c$.

Proof. To construct the desired APV, we place the N MAs with an equal spacing d_x along the x-axis. Hence, the coordinate of the n-th MA is given by $\boldsymbol{t}_n = [(n-1)d_x, 0]^T$, $n \in \mathcal{N}$, and the received SNR at the k-th user can be expressed as

$$\gamma_k(\boldsymbol{T}) = \frac{\beta P_{\max}}{N d_k^2 \sigma_k^2} \left| \sum_{n=1}^{N} e^{j(n-1)d_x a_k} \right|^2 . \forall k \in \mathcal{K}^c. \tag{A5}$$

To reap the maximum beamforming gain in (A5), we can adjust the spacing d_x such that each exponential term in (A5) is equal to unity, for which we have

$$d_x a_k = 2\pi m_k, \forall k \in \mathcal{K}^c, \tag{A6}$$

where m_k is an integer. Note that (A6) is equivalent to find a set of m_k's that satisfy

$$d_x = \frac{\lambda m_2}{\tau_2} = \frac{\lambda m_3}{\tau_3} = \cdots = \frac{\lambda m_K}{\tau_K}. \tag{A7}$$

Next, we show how to construct the desired m_k's satisfying (A7). According to the basic number theory, a rational number can be expressed as the ratio of two relatively prime integers. As each τ_k is a rational number, it can be expressed as $\tau_k = \frac{p_k}{q_k}$, $k \in \mathcal{K}^c$, where p_k and q_k are two relatively prime integers. Let $\hat{m}_k = p_k \prod_{j \neq k} q_j$ and $c_{\max}$ denote the greatest common factor of $\hat{m}_k$, $k \in \mathcal{K}^c$. As such, we can set $m_k = \frac{\hat{m}_k}{c_{\max}}$, $\forall k \in \mathcal{K}^c$ in (A7) and the resulting antenna spacing d_x is

$$d_x^\star = \frac{\zeta \lambda \prod_{k=2}^{K} q_k}{c_{\max}}. \tag{A8}$$

where ζ is the minimum integer that ensures $d_x^\star \geqslant D_{\min}$. By setting $\boldsymbol{t}_n = [(n-1)d_x^\star, 0]^T$, $n \in \mathcal{N}$, we can achieve the maximum beamforming gain at all users. This completes the proof.

* Corresponding author (email: wmei@uestc.edu.cn)

Theorem 1 indicates that even with equal-spacing MAs, the maximum beamforming gain (i.e., N) can be achieved at an arbitrary number of users by simply tuning the antenna spacing to generate the grating lobes based on the users' positions. As the path gain β_k's and the average noise power σ_k^2's are both constant for each user k, the received SNRs at all users can be maximized. Thus, $\boldsymbol{t}_n = [(n-1)d_x^\star, 0]^T$, $n \in \mathcal{N}$ and (A1) should be an optimal solution to (P1) (if constraint (3b) is relaxed). However, Theorem 1 requires all τ_k's to be rational numbers[1)], which may be difficult to be met in practical. Hence, we consider another special case of $N = 2$ and present the following theorem.

Theorem A2. When $N = 2$, for any given $\delta \in (0, 1)$, there must exist an APV $\boldsymbol{T}^\star$ such that

$$\gamma_k(\boldsymbol{T}^\star) \geqslant \frac{\beta P_{\max}}{d_k^2 \sigma_k^2}(1+\delta), \forall k \in \mathcal{K}^c. \tag{A9}$$

Proof. Similar to the proof of Theorem 1, we place the two MAs with a spacing of d_x along the x-axis. By setting $N = 2$, $\boldsymbol{t}_n = [(n-1)d_x, 0]^T$, $n = 1, 2$, the received SNR at the k-th user in (A2) can be simplified as

$$\gamma_k(\boldsymbol{T}) = \frac{\beta P_{\max}}{d_k^2 \sigma_k^2}(1 + \cos a_k d_x), \forall k \in \mathcal{K}^c. \tag{A10}$$

Next, we introduce the following lemma.

Lemma 1 [1]: If a_k's are linearly independent over the set of rational numbers, for any given $\delta \in (0, 1)$, there must exist a $d_x^\star \in \mathbb{N}$ such that

$$\cos a_k d_x^\star > \delta, \forall k \in \mathcal{K}^c. \tag{A11}$$

Note that due to the users' random locations, all a_k's should take an irrational value with the probability of one and thus are linearly independent over the set of rational numbers. As a result, for any given $\delta \in (0, 1)$, by setting $\boldsymbol{t}_n = [(n-1)d_x^\star, 0]^T$, $n = 1, 2$, and applying Lemma 1, (A9) can be achieved. It should be mentioned that as $d_x^\star$ is a positive integer, it should be much greater than the wavelength-level antenna spacing considering the ultra-high THz frequency band. Thus, the minimum spacing constraints in (B1c) should always be satisfied. This completes the proof.

It follows from Theorem 2 by setting $\delta \to 1$, approximately the maximum beamforming gain, i.e., 2, can be attained at all users. This implies that a two-antenna sparse array suffices to generate flexible grating lobes for THz multicasting if the inter-antenna distance can be flexibly adjusted. Both Theorems 1 and 2 indicate that the antenna position optimization offers more degrees of freedom to improve the THz multicast performance over conventional FPAs. It is worth noting that although the above analytical results are derived assuming a LoS channel from the BS to each user, they are also applicable to the case with multi-path BS-user channels, by simply treating each path as a virtual user.

Appendix B Proposed Solution to (P1)

To start with, we introduce an auxiliary variable η. Then, (P1) is equivalent to the following optimization problem:

$$\begin{aligned}
(\text{P1}) \quad & \max_{\eta, \boldsymbol{w}, \boldsymbol{T}} \quad \eta \\
\text{s.t.} \quad & \gamma_k(\boldsymbol{T}) \geqslant \eta, \forall k \in \mathcal{K}, && \text{(B1a)} \\
& \boldsymbol{t}_n \in \mathcal{C}_t, n \in \mathcal{N}, && \text{(B1b)} \\
& ||\boldsymbol{t}_i - \boldsymbol{t}_j||_2 \geqslant D_{\min}, \forall i, j \in \mathcal{N}, i \neq j, && \text{(B1c)} \\
& ||\boldsymbol{w}||_2^2 \leqslant P_{\max}. && \text{(B1d)}
\end{aligned}$$

However, (P1) is still a non-convex optimization problem. To this end, we propose an AO algorithm to decompose (P1) into two subproblems and solve them alternately.

First, we optimize the transmit beamforming $\boldsymbol{w}$ for any given APV $\boldsymbol{T}$. Note that as each channel vector $\boldsymbol{h}_k(\boldsymbol{T})$, $\forall k \in \mathcal{K}$ is fixed, by introducing an auxiliary variable η, (P1) can be simplified as

$$\begin{aligned}
(\text{P2}) \quad & \max_{\eta, \boldsymbol{w}} \quad \eta \\
\text{s.t.} \quad & \boldsymbol{w}^H \boldsymbol{H}_k(\boldsymbol{T}) \boldsymbol{w} \geqslant \eta, \forall k \in \mathcal{K}, && \text{(B2a)} \\
& \boldsymbol{w}^H \boldsymbol{w} \leqslant P_{\max}, && \text{(B2b)}
\end{aligned}$$

where $\boldsymbol{H}_k(\boldsymbol{T}) = \frac{1}{\sigma_k^2} \boldsymbol{h}_k(\boldsymbol{T}) \boldsymbol{h}_k^H(\boldsymbol{T})$, $k \in \mathcal{K}$. However, (P2) is still difficult to solve because the constraints in (B2a) are concave with respect to (w.r.t.) $\boldsymbol{w}$ (instead of convex). To address this challenge, we apply the SCA to transform (P2) into a series of more tractable approximated convex subproblems. Specifically, with a given local point $\boldsymbol{w}_i$, the left-hand side (LHS) of (B2a) can be lower-bounded by its first-order Taylor expansion, i.e.,

$$\begin{aligned}
\boldsymbol{w}^H \boldsymbol{H}_k(\boldsymbol{T}) \boldsymbol{w} &\geqslant \boldsymbol{w}_i^H \boldsymbol{H}_k(\boldsymbol{T}) \boldsymbol{w}_i + 2\text{Re}\left\{\boldsymbol{w}_i^H \boldsymbol{H}_k(\boldsymbol{T})(\boldsymbol{w} - \boldsymbol{w}_i)\right\} \\
&= 2\text{Re}\left\{\boldsymbol{w}_i^H \boldsymbol{H}_k(\boldsymbol{T}) \boldsymbol{w}\right\} - \boldsymbol{w}_i^H \boldsymbol{H}_k(\boldsymbol{T}) \boldsymbol{w}_i \\
&\triangleq \gamma_k^{\text{lb}}(\boldsymbol{T}).
\end{aligned} \tag{B3}$$

1) In the case of irrational numbers, Theorem 1 may also approximately hold by properly truncating each τ_k into a rational number.

Then, by substituting (B3) into (B2a), (P2) in the i-th SCA iteration can be approximated as

$$\text{(P2-}i\text{)} \quad \max_{\eta,\boldsymbol{w}} \quad \eta \quad \text{s.t.} \quad \gamma_k^{\text{lb}}(\boldsymbol{T}) \geqslant \eta, \forall k \in \mathcal{K}, \text{ (B2b)},$$

which is a quadratically constrained quadratic programming (QCQP) problem and thus can be optimally solved by the interior-point algorithm. Next, the SCA proceeds to (P2-$(i+1)$) by setting $\boldsymbol{w}_{i+1}$ as the optimal solution to (P2-i) until the convergence is reached. It can be shown that the computational complexity of solving (P2-i) is in the order of $\mathcal{O}(N^3K^{0.5})$.

Next, we optimize the APV $\boldsymbol{T}$ for any given transmit beamforming vector $\boldsymbol{w}$. In this case, (P1) can be simplified as

$$\begin{aligned} \text{(P3)} \quad & \max_{\eta,\boldsymbol{T}} \quad \eta \\ \text{s.t.} \quad & |\boldsymbol{h}_k^H(\boldsymbol{T})\boldsymbol{w}|^2 \geqslant \eta\sigma_k^2, \forall k \in \mathcal{K}, \qquad \text{(B5a)} \\ & \text{(B1b)}, \text{(B1c)}. \end{aligned}$$

(P3) can be solved by applying a similar sampling-based approach in our previous works [2–4]. Thus, we only outline the main steps. Specifically, we uniformly sample the horizontal/vertical dimension of the transmit region $\mathcal{C}_t$ into M ($M \gg N$) discrete points, with a spacing $\delta_s = A/M$. Then, the coordinate of (i,j)-th sampling point is given by $\boldsymbol{p}_{i,j} = [-\frac{A}{2} + i\delta_s, -\frac{A}{2} + j\delta_s]^T, i,j \in \mathcal{M} \triangleq \{1,2,\cdots,M\}$. Let $\mathcal{P} \triangleq \{\boldsymbol{p}_{i,j} | i,j \in \mathcal{M}\}$ denote the set of all sampling points. Next, we construct a set of initial positions of MAs denoted by $\tilde{\boldsymbol{t}}_n \in \mathcal{P}, n \in \mathcal{N}$. In the n-th iteration of the sequential search, we update the coordinate of n-th MA and fix the coordinates of other $N-1$ MAs. Let $\mathcal{P}_n$ denote the set of all feasible sampling points in the n-th iteration, i.e.,

$$\mathcal{P}_n \triangleq \{\boldsymbol{p} \in \mathcal{P} | ||\boldsymbol{p} - \tilde{\boldsymbol{t}}_m|| \geqslant D, \forall m \in \mathcal{N}, m \neq n\}. \qquad \text{(B6)}$$

Let $\tilde{\boldsymbol{T}}_n \triangleq [\tilde{\boldsymbol{t}}_1, \cdots, \boldsymbol{t}_n, \cdots, \tilde{\boldsymbol{t}}_N]$ denote the collections of N MAs in the n-th iteration. Then, we can optimize $\boldsymbol{t}_n$ by solving the following problem,

$$\begin{aligned} \text{(P3-}n\text{)} \quad & \max_{\boldsymbol{t}_n \in \mathcal{P}_n} \quad \eta \\ \text{s.t.} \quad & |\boldsymbol{h}_k^H(\tilde{\boldsymbol{T}}_n)\boldsymbol{w}|^2 \geqslant \eta\sigma_k^2, \forall k \in \mathcal{K}, \qquad \text{(B7a)} \\ & \text{(B1b)}, \text{(B1c)}, \end{aligned}$$

which can be optimally solved by performing an enumeration over $\mathcal{P}_n$. Denote by $\boldsymbol{t}_n^\star$ the optimal solution to (P3-n). Then, we can update $\tilde{\boldsymbol{t}}_n = \boldsymbol{t}_n^\star$ and proceed to solving (P3-n) via a similar process, which always yields a non-decreasing objective value of (P3). This ensures the convergence of our proposed algorithm. The computational complexity of solving (P3-n) is given by $\mathcal{O}(NM^2)$. Notably, compared to the continuous algorithms for MA position optimization proposed in [5–7], the discrete sampling approach is easier to implement, as it does not require gradient-based calculations and searching.

Based on above, we can alternately solve (P2) and (P3) by applying the SCA technique and the sampling-based method. As both of these two algorithms yield a non-decreasing objective values of (P1), the convergence of AO is guaranteed.

Appendix C Numerical Results

In this appendix, numerical results are provided to demonstrate the efficacy of our proposed algorithm. Unless otherwise specified, the simulation settings are as follows. The operating frequency band is $f = 150$ GHz. The BS is equipped with $N = 4$ MAs. The minimum distance between any two adjacent MAs is $D_{\min} = \frac{\lambda}{2}$. The spacing of the sampling points along x- and y-axes is set as $\delta_s = \frac{\lambda}{25}$. The distances between the BS and all users are assumed to be independent and identically distributed (i.i.d.) random variables following uniform distribution between 10 m and 20 m. The elevation and azimuth AoAs for all users are assumed to be i.i.d. random variables following uniform distribution within $[-\pi/2, \pi/2]$. The BS's maximum transmit power is $P_{\max} = 23$ dBm, and the average noise power is $\sigma_k^2 = \sigma^2 = -80$ dBm, $k \in \mathcal{K}$. All the results are averaged over 100 independent channel realizations.

Moreover, we consider the following benchmark schemes for performance comparison:

1. **MRT**: The BS's transmit beamforming is set as the MRT w.r.t. user 1, i.e.,

$$\boldsymbol{w}(\boldsymbol{T}) = \sqrt{P_{\max}} \frac{\boldsymbol{h}_1(\boldsymbol{T})}{||\boldsymbol{h}_1(\boldsymbol{T})||}, \qquad \text{(C1)}$$

   while the APV is optimized similarly as in Appendix B.

2. **FPA**: The BS's N antennas are deployed symmetrically to the center of the transmit array along the x-axis and separated by the minimum distance $D_{\min}$. The BS's transmit beamforming is optimized similarly as in Appendix B.

3. **Sparse array (SA)**: The BS's N antennas are sparsely and uniformly deployed along the x-axis, with a spacing of $\frac{A}{N}$. The BS's transmit beamforming is optimized similarly as in Appendix B.

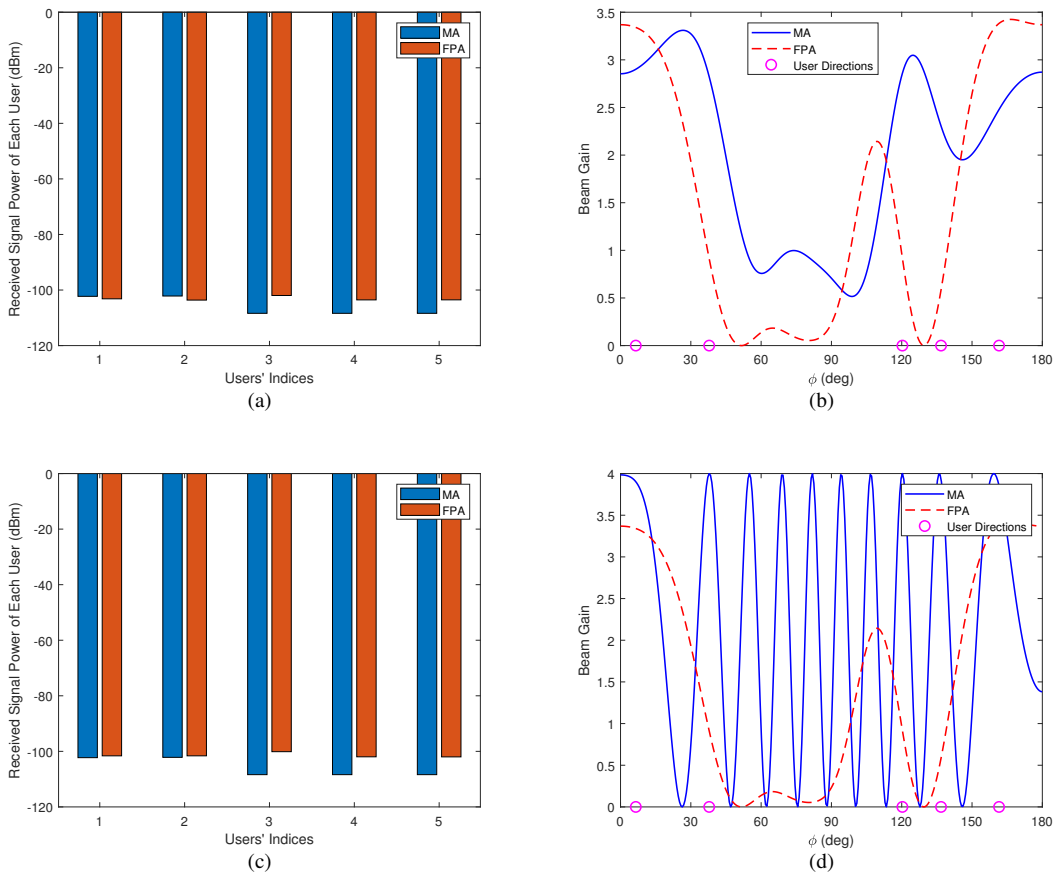

Figure C1 (a) Received signal power of each user and (b) optimized beam patterns by MAs and FPAswith $A = 2\lambda$; (c) received signal power of each user and (d) optimized beam patterns by MAs and FPAs with $A = 8\lambda$.

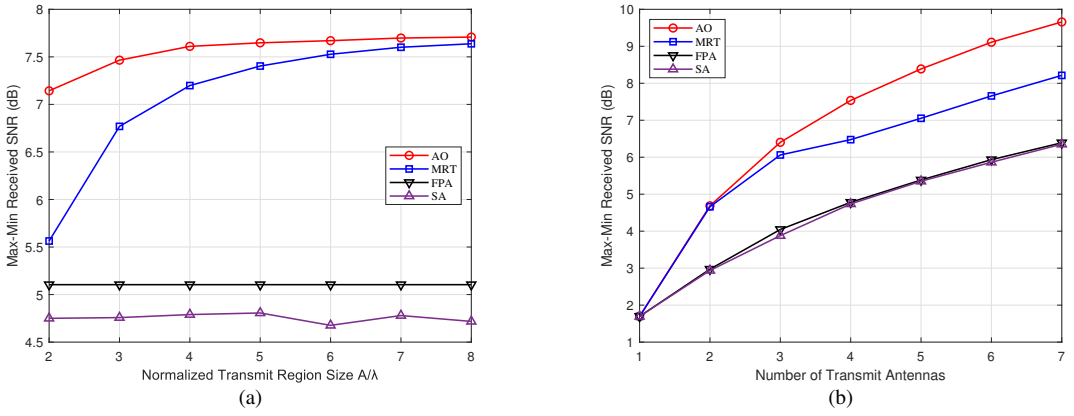

Figure C2 Max-min SNR versus (a) the normalized size of the transmit region, A/λ; (b) the number of transmit MAs.

First, we plot in Figures C1(a) and C1(b) the received signal power of each user and the optimized beam patterns, respectively, by the proposed algorithm and FPAs w/o AS with $A = 2\lambda$. The azimuth AoDs for all users are assumed to be idenntical as $\theta_k = 90°$, $k \in \mathcal{K}$, and the number of users is $K = 5$. It is observed from Figure C1(a) that the max-min received signal power by our proposed algorithm is larger than that by the FPA benchmark. Nevertheless, the received signal powers of certain users (e.g., users 1 and 2) are observed to become smaller with MAs than the FPA benchmark. Moreover, it is observed from Figure C1(b) that the beam gain directed towards certain users may also decrease with MAs compared to FPAs, e.g., user 1 at 6.5°. This is because different users experience varying path losses with the BS, which should be considered in the MA position optimization to achieve the optimal multicast performance. The above observations made from Figures C1(a) and C1(b) imply that in the case of $A = 2\lambda$, MAs play a similar role to conventional transmit

beamforming, primarily for balancing the received signal power at all users.

In Figures C1(c) and C1(d), we show similar results to Figures C1(a) and C1(b) but with $A = 8\lambda$, respectively. In contrast to the above observations, it is observed from Figure C1(c) that all users' received signal powers can be improved with MAs compared to those with the FPA benchmark. Furthermore, it is observed from Figure C1(d) that the beamforming gains for all users are improved as well with MAs. Particularly, the maximum beamforming gain, i.e., $N = 4$, can be approximately attained at all users. It follows that in the case of a large transmit region, it suffices for MAs to maximize the beamforming gain for all users without needing to account for their path losses with the BS as in Figures C1(a) and C1(b).

Next, we plot in Figures C2(a) the max-min received SNRs by different schemes versus the normalized size of the transmit region in each dimension, i.e., A/λ. The total number of users is $K = 6$. It is observed that the max-min received SNRs by all considered schemes (except the FPA and SA benchmark) increase with the transmit region size, as this leads to a larger degree of freedom for antenna position optimization. In particular, our proposed AO algorithm is observed to outperform all other benchmarks. Nonetheless, as A increases, the performance gap between MRT and AO reduces, which is consistent with our theoretical analysis. It is also observed that the SA benchmark may even yield a worse performance compared to the FPA benchmark. This is because the SA may not be able to generate high-gain grating lobes towards the considered directions of the users given its fixed inter-antenna spacing.

Lastly, we plot the max-min received SNRs by different schemes versus the number of MAs in Figures C2(b), with $A = 4\lambda$. It is observed that the max-min SNRs by all considered schemes increase with the number of MAs. This is expected, as more antennas lead to a higher beamforming gain to enhance the multicast performance. Moreover, it is observed that to achieve the same max-min received SNR, the proposed scheme requires fewer antennas than FPA benchmark. For instance, to achieve a max-min SNR of 6 dB, the proposed scheme uses only 3 antennas, whereas the FPA benchmark uses 7 antennas. This suggests that MAs can significantly reduce the hardware cost and power consumption of conventional THz BSs with FPAs. It is also observed that the performance gain of the proposed scheme over other benchmarks becomes more significant with an increasing number of MAs. This implies that continuous antenna movement yields a more substantial gain for multicasting with a large number of antennas.

References

1 Leshem A. and Erez U. The interference channel revisited: Aligning interference by adjusting antenna separation. IEEE Trans. Signal Process, 2021 69: pp. 1874-1884
2 Mei W D, Wei X, Ning B Y, et al. Movable-antenna position optimization: A graph-based approach. IEEE Wireless Commun. Lett, 2024, 13: 1853-1857
3 Wei X, Mei W D, Wang D. et al. Joint beamforming and antenna position optimization for movable antenna-assisted spectrum sharing. IEEE Wireless Commun. Lett, 2024, 13: 2502-2506
4 Mei W D, Wei X, Liu Y J, Ning B Y, and Chen Z, Movable-antenna position optimization for physical-layer security via discrete sampling. Proc. IEEE Global Commun. Conf., 2024, 4739-4744
5 Kang N J. Deep learning enabled multicast beamforming with movable antenna array. IEEE Wireless Commun. Lett, 2024, 13: 1848-1852
6 Gao Y, Wu Q Q and Chen W. Joint transmitter and receiver design for movable antenna enhanced multicast communications. IEEE Trans. Wireless Commun, 2024, 23: 18186-18200
7 Wang D, Mei W D, Ning B Y, and Chen Z. Flexible beam coverage optimization for movable-antenna array. Proc. IEEE Global Commun. Conf., 2024, 4903-4908